



---

# Symmetric inheritance of parental histones governs epigenome maintenance and embryonic stem cell identity

---

In the format provided by the authors and unedited

---

# 1 **Supplementary Methods**

2

## 3 **Genome editing**

4 MCM2-2A mESCs were generated by changing tyrosine 81 and 90 to alanine residues using  
5 transcription activator-like effector nucleases (TALENs) and a recombination reporter  
6 plasmid<sup>1</sup>. TALENs were assembled using the Golden Gate TALEN cloning kit<sup>2</sup> (addgene  
7 #1000000024) and acceptor vectors SV40-ELD and SV40-KKR<sup>1</sup>. Cells were transfected with  
8 400 ng TALEN-EED, 400 ng TALEN-KKR, 100 ng recombination reporter (pRR-Puro or  
9 pRR-EGFP) and 1.1 µg single-stranded oligonucleotide donor #1 (IDT) (Supplementary  
10 Table 3) using Lipofectamine 3000 reagent (Invitrogen, L3000015). For the experiment with  
11 the Puromycin reporter, cells were selected 24 hours post-transfection with Puromycin (2  
12 µg/mL) for 36 hours and seeded sparsely on a 10 cm dish. After one week of culture,  
13 individual clones were picked manually with a pipette and each clone was distributed  
14 between two 96-well plates (one plate for genotyping, one plate for expansion). For the  
15 experiment with the EGFP reporter, GFP-positive cells were sorted into 96-well plates (BD  
16 FACSAria III cell sorter) 24 hours post-transfection and cultured for one week before  
17 expansion and genotyping. For PCR genotyping, cells were washed with PBS and lysed by  
18 adding 20 µL of ESC DNA lysis buffer (10 mM Tris-HCl pH 8.0, 0.5 mM EDTA, 0.5 %  
19 Triton-X100) and 0.5 µL of Proteinase K (20 mg/mL; Sigma, P6556) directly into the wells,  
20 followed by incubation at 55 °C for 1.5 hours. Proteinase K was inactivated by incubation at  
21 95 °C for 10 min and lysates were directly used for PCR. The genomic region surrounding  
22 the sites to be mutated was amplified in a 12 µL PCR reaction using OneTaq Hot Start 2x  
23 Master Mix (NEB, M0484L) and primers #1 and #2 (TAG Copenhagen) (Supplementary  
24 Table 3). Half of the PCR product was digested with restriction enzyme AccI (NEB, R0161L)  
25 in a 20 µL reaction at 37 °C for 1 hour and was analysed by agarose gel electrophoresis

1 together with the undigested product. Positive clones were verified by sequencing with  
2 primer #3 (TAG Copenhagen) (Supplementary Table 3). Clones which did not carry the  
3 MCM2 mutations were kept as control clones. Note that WT#1 refers to the parental cell line,  
4 while WT#2-8 refers to negative clones from the genome editing.

5

6 MCM2-R mESCs were generated by reversing the mutations back to wild-type sequence in  
7 two independent MCM2-2A clones, MCM2-2A#1 and MCM2-2A#2. Genome editing was  
8 performed as described above, except that CRISPR-Cas9 was used instead of TALENs. Cells  
9 were transfected with 900 ng of SpCas9(BB)-2A-Puro (PX459) V2.0 plasmid (addgene  
10 #62988) containing sgRNA #1, 100 ng of recombination reporter (pRR-Puro) and 1 µg of  
11 single-stranded oligonucleotide donor #2. PCR genotyping was performed as described  
12 above. Oligonucleotide sequences are listed in Supplementary Table 3.

13

14 POLE4 KO mESCs were generated by CRISPR-Cas9 using the SpCas9(BB)-2A-Puro  
15 (PX459) V2.0 plasmid (addgene #62988) with sgRNA #2 and sgRNA #3 (Supplementary  
16 Table 3), which target the Pole4 gene at the beginning of exon 1 and the end of exon 2,  
17 respectively. Cells were transfected using Lipofectamine 3000 reagent (Invitrogen,  
18 L3000015) using 0.5 µg of each sgRNA-plasmid. Cells were sparsely seeded on a 10 cm dish  
19 24 hours post-transfection and selected with Puromycin (2 µg/mL) for 48 h. Thereafter, cells  
20 were expanded and genotyped with primers #4, #5 and #6 (as described above)  
21 (Supplementary Table 3). Positive clones were analysed by Sanger sequencing with primers  
22 #4 and #5 (IDT) and Pole4 knockout was confirmed by Western Blot. For preparation of  
23 whole cell extracts, cells were washed with PBS and lysed on plate by adding Laemmli buffer  
24 (50m Tris-HCl pH 6.8, 100 nM DTT, 2% SDS, 10% Glycerol, Bromphenol blue), transferred  
25 to 1.5 mL tubes and subsequently incubated with Benzonase (25 U, Sigma, 70746-3) at 37 °C

1 for 1h, followed by heat denaturation. Samples were separated on a 4-12% NuPAGE Bis-Tris  
2 protein gel (Invitrogen, NP0321BOX) and transferred to a Nitrocellulose membrane  
3 (Amersham, 15239794). Membrane was blocked for 1 h in 5% skim milk (Sigma, 70166)  
4 with PBST and incubated with primary antibodies overnight (Supplementary Table 3).  
5 Following 3 PBST washes, membrane was incubated with peroxidase-conjugated secondary  
6 antibody for 1 h. Blots were incubated for 5 min with SuperSignal™ West Pico PLUS  
7 chemiluminescent solution (Thermo Scientific, 34580) and visualized on (ImageQuant LAS  
8 4000, GE Healthcare).

9

### 10 **Pulse-SILAC mass spectrometry**

11 Cells were adapted to light SILAC media. For SILAC media, the DMEM and FBS described  
12 above for serum+LIF media were replaced with DMEM for SILAC (Thermo Fisher, 88364)  
13 and dialyzed FBS (Thermo Fisher, 6400-044), and media was supplemented with light lysine  
14 (K0; Sigma, L8662) at 798  $\mu$ M and light (R0; Sigma, A8094), medium (R6) or heavy (R10)  
15 arginine at 398  $\mu$ M (Cambridge Isotope Laboratories, CLM-2265-H-PK or CNLM-539-H-  
16 PK). Cells were seeded in light SILAC media in 15 cm dishes ( $4 \times 10^6$  cells per dish, 1 dish  
17 per time point and cell line). On the following day, cells were pulsed with medium SILAC  
18 media for 3 hours to label new histones, followed by a chase with heavy SILAC media to  
19 track old (light) and new (medium) histone dynamics throughout one cell cycle (see scheme  
20 in Extended Data Fig. 1a). Samples were harvested immediately after the pulse (0 h) and at  
21 several chase time points (4 h, 8 h, 12 h and 16 h). Dishes were washed once with PBS during  
22 media changes. For sample collection, cells were trypsinized, washed twice in cold PBS,  
23 snap-frozen and stored at -80 °C until further use. Cell pellets were acid extracted according  
24 to standard protocols. Extracted chromatin pellets were air-dried, stored at -20 °C until all  
25 replicates were collected, and shipped on dry ice to EpiQMAx GmbH. Further sample

1 preparation and MS analysis were performed according to the EpiQMAx GmbH protocols.  
2 Briefly, acid extracted histones were resuspended in Lämmli buffer and separated by a 14-  
3 20% gradient SDS-PAGE, stained with Coomassie (Brilliant blue G-250, 35081.01). Protein  
4 bands in the molecular weight range of histones (15-23 kDa) were excised as single  
5 band/fraction. Gel slices were destained in 50% acetonitrile/50mM ammonium bicarbonate.  
6 Lysine residues were chemically modified by propionylation for 30 min at RT with 2.5%  
7 propionic anhydride (Sigma, 8.00608) in ammonium bicarbonate, pH 7.5. Subsequently,  
8 proteins were digested with 200ng of trypsin (Promega, V5111) in 50mM ammonium  
9 bicarbonate overnight and the supernatant was desalted by C18-Stagetips (reversed-phase  
10 resin) and carbon Top-Tips (Glygen, TT1CAR) according to the manufacturer's instructions.  
11 After desalting, the eluent was speed vacuumed until dryness and stored at -20°C until MS  
12 analysis.

13

14 *LC-MS analysis:* Peptides were re-suspended in 17 µl of 0.1% TFA. A total of 5.0 µl were  
15 injected into a nano-HPLC device (Thermo Fisher Scientific, UltimateNano3000) using a  
16 gradient from 4% B to 90% B (solvent A 0.1% FA in water, solvent B 80% ACN, 0.1% FA  
17 in water) over 90 min at a flow rate of 300 nl/min in a C18 UHPCL column (Thermo Fisher  
18 Scientific, 164534). Data was acquired in PRM positive mode using a Q Exactive HF  
19 spectrometer (Thermo Fisher Scientific) to identify and quantify specific N-terminal peptides  
20 of histone H3 and histone H4 proteins and their PTMs. One survey MS1 scan and 9 MS2  
21 acquisitions precursor m/z value in the inclusion list was performed. MS1 spectra were  
22 acquired in the m/z range 250-1600 with resolution 30,000 at m/z 400 (AGC target of  $3 \times 10^6$ ).  
23 PRM spectra were acquired with resolution 15,000 to a target value of  $2 \times 10^5$ , maximum IT  
24 60ms, isolation 2 window 0.7 m/z and fragmented at 27% normalized collision energy.

1 Typical mass spectrometric conditions were: spray voltage, 1.5kV; no sheath and auxiliary  
2 gas flow; heated capillary temperature, 250°C.

3

#### 4 **Mass spectrometry data analysis**

5 *Pulse-SILAC*: Raw files were searched with the Skyline software<sup>3</sup> against histone H3, H4 and  
6 H2A almost unmodifiable peptides KLPFQR, DNIQGITKPAIR and IIPR, respectively. The  
7 MS1 signals of these peptides were extracted with a precursor mass tolerance of 5 ppm. The  
8 chromatogram boundaries of +2 and +3 charged peaks were validated and the “Total Area  
9 MS1” under the first 4 isotopomers was used for relative quantification and comparison  
10 between the label groups light, medium and heavy at each time point.

11

12 *Histone PTMs*: Raw files were searched with the Skyline software<sup>3</sup> against histone H3 and  
13 H4 peptides and their respective PTMs with a precursor mass tolerance of 5 ppm. The  
14 chromatogram boundaries of +2 and +3 charged peaks were validated and the Total Area  
15 MS1 under the first 4 isotopomers was extracted and used for relative quantification and  
16 comparison between experimental groups. The Total Area MS1 of co-eluting isobaric  
17 peptides (i.e., H3K36me3 and H3K27me2K36me1) was resolved using their unique MS2  
18 fragment ions. The averaged ratio of analogous ions (i.e., y7 vs y7) were used to calculate the  
19 respective contribution of the precursors<sup>4</sup> to the isobaric MS1 peak.

20 Relative abundances (percentages) were calculated as in the following example for H3K18  
21 acetylation:

$$22 \quad \%H3K18ac = (H3K18ac\_K23un + H3K18ac\_K23ac) / (H3K18un\_K23un +$$
$$23 \quad H3K18ac\_K23unmod + H3K18un\_K23ac + H3K18ac\_K23ac)$$

24 where “ac” indicates acetylation and “un” indicates unmodified.

25

## 1 **Genomic data analysis**

### 2 **SCAR-seq**

3 *Data processing:* Reads were processed and mapped (mm10) with the ENCODE ChIP-seq  
4 pipeline as described below. The resulting processed bam files were split into forward and  
5 reverse strands according to the SAM flag, using samtools view (version 1.5) -F 20 and -f 16,  
6 respectively.

7

8 *Histone partition:* Signal was computed using the analysis scripts related to<sup>5</sup>. For each strand  
9 the SCAR normalized signal (CPM) was computed in 1kb bins and smoothed in a uniform  
10 blur considering the neighbouring 30 bins on each side. For each 1kb window, the signal  
11 from its corresponding SCAR input was subtracted and negative values were set to zero.  
12 Input corrected windows with CPM < 0.3 on both strands were filtered out and not  
13 considered for further analyses. The final partition score for each 1kb window was calculated  
14 as:

$$15 \text{ Partition} = (F - R)/(F + R)$$

16 where F and R correspond to the number of normalized and input-corrected reads for the  
17 forward and reverse strand, respectively. The partition value relates to the ratio of histones  
18 with a specific modification being segregated to the nascent forward (Partition > 0) or nascent  
19 reverse (Partition < 0) strand within each window respectively. Extreme partition ratios  
20 (values > 0.9999 quantile or < 00001 quantile) were set to the quantile value. Partition signal  
21 from each replicate was analysed separately for statistical robustness analyses within each  
22 mark and timepoint, while the average partition signal from both replicates was used for  
23 visualization purposes.

24

1 *Okazaki-seq*: Replication fork directionality (RFD) scores and filtered initiation zones (IZs)  
2 for mESC were taken from<sup>5</sup> and used as focus points to define replication via leading or  
3 lagging strand mechanism. The RFD score in *Okazaki-seq* is calculated like SCAR-seq  
4 partition scores but subtracting the forward (F) strand signal from the reverse (R) strand  
5 signal instead:  $RFD = (R - F)/(F + R)$   
6 For each mark (H3K4me3, H3K27me3 and H3K27ac) as well as SUZ12, only IZs zones  
7 within 100kb of WT ChIP-seq defined peaks were used for further analysis. Initiation zone  
8 edges, where the RFD reach local extrema, were determined within 100 kb upstream and  
9 downstream of the initiation zone, by selecting the location with minimum and maximum  
10 RFD value, respectively. A window size of 200 kb around each initiation zone was chosen  
11 based on the average initiation zone size (from upstream to downstream initiation zone  
12 edge) (mean size = 112 kb) and the distances to neighbouring initiation zones (mean distance  
13 = 359 kb). This left a total of  $n = 2076$ ,  $n = 2040$  and  $n = 2063$  IZs used for downstream  
14 analyses in H3K27me3, H3K4me3, H3K27ac marks respectively, and  $n = 1241$  IZs for  
15 SUZ12.  
16 The difference in SCAR-seq partition ratios at initiation zone edges between leading and  
17 lagging enriched strands were tested with a Wilcoxon signed-rank test. The test was  
18 performed between each pair of SCAR-seq samples, taking all 1kb windows with sufficient  
19 coverage, between 10 and 90kb from its nearest initiation zone but not further away than  
20 10kb from the two RFD extrema at both sides from the initiation zone. To compare partition  
21 values on both sides of the initiation zones, an adjusted partition score was computed by  
22 negating the partition values of all windows upstream of the initiation zone. For H3K27ac  
23 analyses, unstranded signal over 200bp bins was computed using the `windowCounts` function  
24 within the `csaw` R package<sup>6</sup> after filtering windows with FC over input above 1.5 in at least  
25 one of the four clones.



1 *Replication timing profiles:* Mouse ESC RT<sup>7</sup> data were downloaded from  
2 <https://www.replicationdomain.com/database.php#> (accession Int14787930) and lifted from  
3 mouse mm8 to mouse build mm10 using liftOver. Replication domains were classified as  
4 early ( $\log_2FC > 0$ ) or late ( $\log_2FC < 0$ ) and further split into early (late) and mid-early (mid-  
5 late) based on their median  $\log_2FC$  values. IZs were then annotated with replication timing  
6 by their nearest replication domain classification.

7

## 8 **Quantitative ChIP-seq**

9 *Data processing:* For peak focused analysis reads were processed according to the ENCODE  
10 ChIP-seq pipeline (version 1.3.6): adapters and low-quality reads were filtered with cutadapt  
11 (version 2.5), reads were mapped to a hybrid mouse (mm10) and fly (dm3) genome with bwa,  
12 duplicate reads were removed with picard (version 2.20.7), ENCODE mm10 blacklist regions  
13 were masked and only reads with mapping quality above 30 were considered for further  
14 downstream analyses. To obtain reference-adjusted reads per-million (RRPMs), spike-in  
15 normalization factors for each sample were calculated as  $in^8: 1 / Nd$  where Nd is the number  
16 of exogenous (dm3) reads per million. To calculate the total histone levels in each sample,  
17 the total number of unique reads (uniquely and multi mapping) were multiplied by their  
18 corresponding spike-in normalization factors.

19 Read coverage for all ChIP-seq samples were computed from filtered bam files using  
20 deepTools multiBamSummary (version 3.0) in bins of 1kb and data was fed to deepTools  
21 plotCorrelation for creating pairwise Pearson correlations heatmaps, with all biological  
22 replicates showing high correlation. Visualization tracks for ChIP-seq data were created using  
23 deeptools (version 3.0) bamCompare, averaging both replicates after multiplying them by  
24 their corresponding spike-in scaling factors. For analysis of chromatin marks over repeat  
25 subfamilies, filtered reads were mapped (mm10) using STAR (version 2.7.1a) with the same

1 parameters as for RNA-seq but with the addition of `--alignIntronMax 1` and `alignEndsType`  
2 `EndToEnd`. Histone level quantification over repeat subfamilies was obtained with the same  
3 program, parameters, and annotations as for RNA-seq (see below).

4

5 Peak calling was performed with `macs2` (version 2.2.4<sup>9</sup>), narrow peaks for H3K4me3,  
6 H3K27ac and SUZ12 with parameters `--nomodel -p 0.05`, while broad peaks (H3K27me3 and  
7 H3K9me3 and all external native ChIP datasets were called with `danpos` (version 2.2.4)<sup>10</sup>  
8 dregion with default parameters. All other broad PTMs from external crosslinked datasets  
9 were called with `macs2` using parameters `--nomodel --broad -p 0.01 --broad-cutoff 0.1`, using  
10 as controls their corresponding pooled inputs from all replicates. For each clone a confident  
11 set of peaks was obtained by calling peaks on the pooled replicates and keeping peaks in the  
12 pooled set that overlapped by at least 50% bp in at least 2 replicates. To obtain a list of  
13 confident nucleation sites, a SUZ12 strict set of peaks for each clone was obtained by  
14 irreproducible discovery rate (IDR)<sup>11</sup> analyses with cutoff of  $IDR < 0.05$ .

15 External datasets:

16 - H2AK119ub1 (GSE132752: GSM3891343 and GSM3891344, inputs GSM3891350,  
17 GSM3891351<sup>12</sup>)

18 - H3K27me1 and H3K27me2 (GSE127117: GSM3625691 and GSM3625689, input  
19 GSM3625706<sup>13</sup>)

20 - H3K36me2 (GSE126864: SRR8601997, SRR86019978, SRR86019979, inputs  
21 SRR8602003, SRR8602004, SRR8602005<sup>14</sup>)

22 - H3K36me3 (ENCODE: GSM6373350 and GSM6373351, inputs GSM4051038,  
23 GSM4051039)

24

1 *Data analysis:* All data analyses was performed using R (version 3.4.3) and Bioconductor  
2 (version 3.14). Peak overlap analysis was performed with the package ChIPpeakAnno  
3 (version 3.4.2) R package, peaks were annotated using a modified annotatePeak function in  
4 the ChIPseeker (version 1.26.2) R package with default parameters and a txdb object created  
5 from the GENCODE annotations. Association of gained or lost peaks in MCM2-2A vs WT  
6 with peak annotations was tested with Fisher's exact test. The package csaw was used to  
7 compute ChIP signal over genome-wide bins of sizes 5KB for broad marks (H3K27me3 and  
8 H3K9me3) and 2.5KB was used for narrow marks (H3K4me3, H3K27ac, SUZ12). Bins that  
9 weren't  $\log_2(1.5)$  over input in at least one clone were filtered out. Differential occupancy  
10 (DO) of bins was performed with edgeR using quasi-likelihood test and bins were deemed  
11 significant if  $FDR < 0.1$ . DO of ChIP-seq at the promoter levels. To compute ChIP signal  
12 over annotated gene promoters, for each TSSs surrounding region counts were obtained using  
13 the regionCounts function of the csaw package. Different region sizes were tested (+/-1kb,  
14 2kb, 3kb, 5kb and 10kb) and for each PTM the best size was selected based on the highest  
15 correlation with gene expression (see below). Differential binding at TSSs was performed  
16 with edgeR (version 3.32.1) using quasi-likelihood test and promoters were deemed  
17 significant with cutoff  $FDR < 0.01$ . ChIP-seq signal over gene levels was obtained using the  
18 overlapResults function of csaw. A combined p-value and  $\log_2FC$  was obtained using the  
19 results from the DO TSSs analyses. After correlating gene-level ChIP-seq with RNA-seq  
20  $\log_2FC$ , we found the optimal regions size surrounding the TSSs to be: H3K27ac = +/-10KB,  
21 H3K27me3 = +/-1kb, H3K9me3 = +/-5kb, H3K4me3 = +/-1kb and SUZ12 = +/-1kb.  
22  
23 ChIP signal over repeat subfamilies was quantified with the TEcount program (see RNA-seq  
24 methods) on the STAR aligned bam files. Differential ChIP signal between MCM2-2A and  
25 WT samples was computed using DESeq2 (version 1.30.1) ,  $\log_2$  Fold changes were shrunk

1 using the apeglm method<sup>15</sup> for visualization in order to give less weight to subfamilies with  
2 low counts. Global increase of histone mark levels (RRPMs) in MCM2-2A clones vs WT  
3 clones was tested with an upper-tail Wilcoxon signed rank test.

4

5 *Promoter chromatin state analysis:* Chromatin states were defined for promoters, defined by  
6 annotated TSSs (GENCODE vM23), whose genes were supported by RNA-seq expression  
7 data in any of the considered clones. The presence of ChIP-seq peaks of H3K4me3,  
8 H3K27me3, H3K9me3 and H3K27ac called in WT#1 within 1kb of promoters were  
9 considered. Association of gene DE status with WT chromatin state was tested using Fisher's  
10 exact test comparing the frequency of a state in DE promoters versus all other expressed  
11 promoters.

12

### 13 **RNA-seq**

14 *Data processing:* Sequences were trimmed for adapters and filtering for low quality reads  
15 was performed with trimmomatic (version 0.39) with default parameters. Mapping (mm10)  
16 was performed with STAR (version 2.7.1a) with parameters `-twopassMode Basic -`  
17 `twopass1readsN -1 -alignSJDBoverhangMin 10` and multimapping parameters `-`  
18 `winAnchorMultimapNmax 200 -outFilterMultimapNmax 100` for further repeats  
19 quantification as suggested in<sup>16</sup>.

20

21 *Transcribed repetitive elements:* Quantification of repeat subfamilies was performed on the  
22 processed bam files with the program Tecount (version 2.1.3), part of the Tetrascripts  
23 package<sup>17</sup>, using the provided curated repeat annotations for mm10  
24 ([http://labshare.cshl.edu/shares/mhammelllab/www-data/TEtranscripts/TE\\_GTF/](http://labshare.cshl.edu/shares/mhammelllab/www-data/TEtranscripts/TE_GTF/)). To obtain

1 count values at the loci level, the Telocal (version 1.1.1) program (also part the Tetoothkit suit  
2 of tools) was used, using the same parameters as Tecount.

3

4 *Data analysis:* Differential expression analysis between MCM2-2A and WT clones was  
5 performed with Deseq2 accounting for batch effects detected in PCA analysis, product of  
6 different sequencing runs. Differentially expressed (DE) genes/repeat subfamilies were  
7 defined as those with  $|FC| > 1.5$  and  $FDR < 0.01$ . Heatmaps were created with the pheatmap  
8 R package, GO term functional enrichment was performed with the package clusterProfiler<sup>18</sup>  
9 (version 3.18.1). Gene Set Enrichment Analysis (GSEA)<sup>19</sup> was preformed using GSEA  
10 software (version 4.0.3) to test the enrichment of gene sets specifically expressed in early  
11 embryonic or 2C-like cells<sup>20-22</sup> in MCM2-2A DE genes. Raw fastq files for SUZ12-KO<sup>23</sup>  
12 (GSE127804), SETDB1-KO<sup>24</sup> (BioProject PRJNA544540) and SUV39H1/2-dKO<sup>25</sup>  
13 (GSE57092) experiments were downloaded and processed in the same way as MCM2-2A  
14 RNA-seq to obtain lists of DE genes and repeats used for overlap analyses.

15

## 16 **scRNA-seq**

17 *Data processing:* Data processing: 3' cell multiplexing data was converted with Cell Ranger  
18 (version 6.0.2) to acquire raw reads (cellranger mkfastq) and subsequently sparse matrices  
19 (cellranger multi) based on GENCODE vM23 transcriptome annotations. To identify cell  
20 doublets and outliers all samples were first log-normalized and scaled individually via Seurat  
21 (version 4.0.4). Integration of all samples was based on identifying anchors by mutual nearest  
22 neighbours after concerted dimensionality reduction across datasets via diagonalized  
23 canonical correlation analysis (CCA<sup>26</sup>). Cells corresponding to doublets were identified with  
24 DoubletFinder (version 2.0.3) with the doublet formation rate retrieved from Cell Ranger's  
25 estimates for homotypic doublets. Cells were defined as outliers when  $>10\%$  of a cell's total

1 number of reads were mapped to mitochondrial genes. To perform RNA velocity analyses,  
2 the 3' cell multiplexing data was processed with velocity (version 0.17.17) based on read  
3 alignments derived from Cell Ranger to acquire sparse matrices for both spliced and  
4 unspliced transcripts per sample. The resulting loom files were read with SeuratWrappers  
5 (version 0.3.0) and the velocity-derived Seurat objects were filtered against cells identified as  
6 doublets or outliers. Standard processing for all samples included log-normalization and  
7 variable feature detection before and scaling, dimensionality reduction (i.e., PCA, UMAP)  
8 and cluster identification before and after CCA-based sample integration. Clustree (version  
9 0.4.3) was used to optimise the resolution of detected clusters.

10

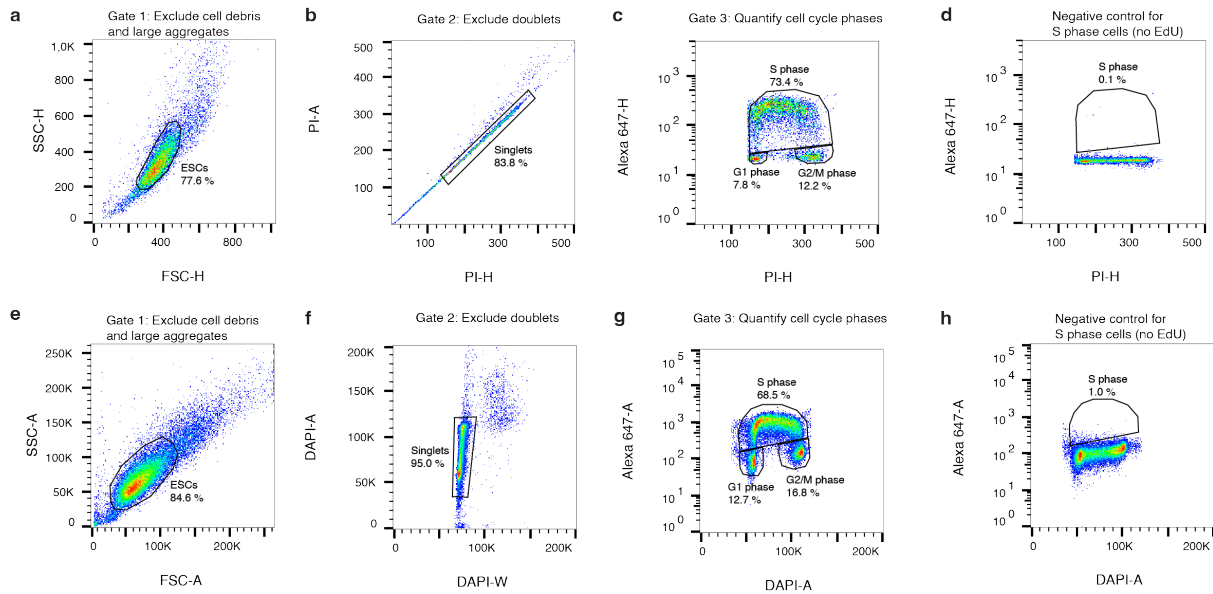
11 *Data analysis:* Integrated Seurat objects were converted via SeuratWrappers into cell data set  
12 objects amenable for monocle3 (version 1.0.0) to learn pseudotime trajectories separately for  
13 WT, MCM2 and MCM2-R samples. Transcriptome velocities were acquired based on  
14 SeuratWrappers, velocity.R (version 0.6) and the velocity-derived transcript counts. Custom  
15 R objects and functions were devised to visualize velocities on UMAP embeddings via  
16 ggplot2 (version 3.3.5). Cells were further assigned cell cycle phases via the cyclone function  
17 in scran (version 1.18.7) based on mouse cell cycle markers provided by that package. All  
18 expression values for individual genes per cell in the UMAP embedding and in the density  
19 plots were Seurat-derived log-normalized counts after CCA-integration for spliced  
20 transcripts. Quantification of transcribed repetitive elements was obtained using the scTE  
21 program (version 1.0)<sup>27</sup>.

22

23

24

25



1

2 **Supplementary Fig. 1. Flow cytometry gating strategy for cell cycle analysis.** Representative

3 example of gating strategy for experiments with MCM2-2A ESCs (a-d) shown in Extended Data Fig.

4 1d-f, and for experiments with POLE4 KO ESCs (e-h) shown in Extended Data Fig.8b. For MCM2-

5 2A experiments, cells were stained with Propidium Iodide (PI) to visualize DNA content and analyzed

6 on a FACS Calibur instrument. For POLE4 KO experiments, cells were stained with DAPI to

7 visualize DNA content and analyzed on a LSR Fortessa instrument. Note that the overall gating

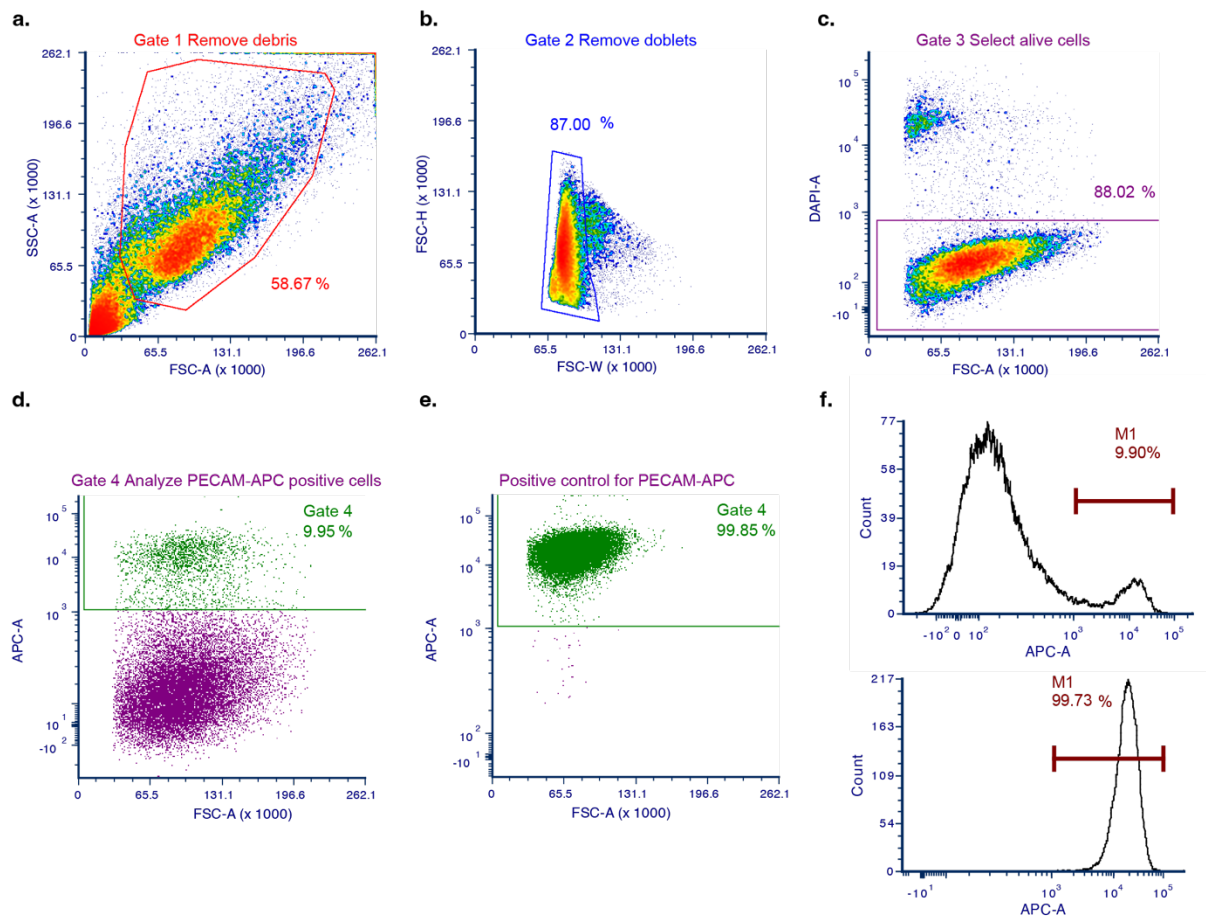
8 strategy was the same for all experiments: The main cell population was selected by excluding cell

9 debris and large aggregates (a, e), followed by selection of singlets (b, f). The cell cycle distribution

10 was then analysed based on EdU incorporation and DNA content (c, g), where a “no EdU”-sample

11 was used as negative control for S phase cells (d, h).

12



1  
2  
3  
4  
5  
6  
7  
8  
9  
10  
11

**Supplementary Fig. 2. Flow cytometry gating strategy for neuronal differentiation.**

Representative example of gating strategy for PECAM positive cells during neuronal differentiation shown in Fig. 6b and Extended Data Fig. 10a. The main cell population was selected by excluding cell debris and large aggregates (a), followed by selection of singlets (b), followed by a selection of live cells or DAPI negative cells (Cells were stained 1:10000 for DAPI) (c). Followed by the analysis of PECAM positive populations. Cells were stained 1:200 for PECAM-APC. Negative and positive controls (e) were used to select the proper PECAM gating. In (f) examples of two histograms showing one clone having only 10% PECAM positive cells and another clone having 100% PECAM positive cells.



1 **Supplementary Table 1. Sequencing data generated in this study.**

2 The file contains information about all SCAR-seq, ChIP-seq, RNA-seq and single-cell RNA-  
3 seq samples, which were generated in this study. Datasets are grouped according to  
4 experiment.

5

6 Column description:

- 7 1. Sample ID (identical to GEO sample ID)
- 8 2. Experiment ID
- 9 3. EdU pulse length (min)
- 10 4. Cell line name (internal ID in Groth lab)
- 11 5. Clone name (cell line ID used in this study)
- 12 6. Replicate name
- 13 7. Number of mapped reads
- 14 8. Fraction of reads mapped
- 15 9. Fraction of duplicated reads (before quality filtering)
- 16 10. Number of mapped reads after quality filtering and de-duplication
- 17 11. Non-redundant fraction (NRF) for library complexity QC
- 18 12. Normalized strand cross-correlation coefficients (NSC) for enrichment QC
- 19 13. Relative strand cross-correlation coefficients (RSC) for enrichment QC
- 20 14. Number of detected cells
- 21 15. Number of filtered cells
- 22 16. Average number of spliced reads per filtered cell
- 23 17. Average number of spliced features per filtered cell
- 24 18. Mode of sequencing

25

26

1 **Supplementary Table 2. Antibodies used in this study.**

Name	Supplier	Catalog number	Assay	Concentration
H3K27me3	Cell signaling	9733S	ChIP	10 $\mu$ L/10 $\mu$ g chromatin for native ChIP 5 $\mu$ L/10 $\mu$ g chromatin for crosslinked ChIP
H3K4me3	Cell signaling	9751S	ChIP	10 $\mu$ L/10 $\mu$ g chromatin
H3K9me3	abcam	ab176916	ChIP	1 $\mu$ g/10 $\mu$ g chromatin
H3K27ac	Epicypther	13-0045	ChIP	2.5 $\mu$ g/10 $\mu$ g chromatin
H4K20me0	abcam	ab227804	ChIP	1 $\mu$ g/10 $\mu$ g chromatin
SUZ12	Cell signaling	3737S	ChIP	2.5-5 $\mu$ L/10 $\mu$ g chromatin
Cytokeratin7	Santa Cruz	sc70936	IF	1:200
Gata6 XP	Cell signaling	5851	IF	1:200
Nanog	eBioscience	14-5761	IF	1:200 on cells 1:50 on embryos
Otx2	R&D	AF1979	IF	1:150
Pecam APC conj (CD31)	BD Pharmingen	551262	Flow cytometry	1:400
Tuj1	Covance	mms-435p	IF	1:500
Tubulin	Abcam	ab6160	Western Blot	1:10000
POLE4	Gift from S. Boulton <sup>28</sup>	N/A	Western Blot	1:1000

2

3

4

5

6

7

8

9

10

11

1 **Supplementary Table 3. TALEN and oligonucleotide sequences related to genome**  
2 **editing.**

Name	Experiment	Sequence
TALEN-EED	MCM2-2A generation	HD NG HD NG NG NN HD NI NN NI NN NI HD NG NI HD HD NN NG (targets: CTCTTGCAGAGACTACCGT)
TALEN-KKR	MCM2-2A generation	HD HD HD NG HD NN NN HD HD NG HD NN NG NI NN NI HD NI NG (targets: CCCTCGGCCTCGTAGACAT)
sgRNA #1	MCM2-R generation	GCGACATCGAGCTCCGGAAT
sgRNA #2	POLE4-KO generation	CACGTTTCGGGAGGGGATGG
sgRNA #3	POLE4-KO generation	CTCTACCCAAATCTCTCCTC
Oligonucleotide donor #1*	MCM2-2A generation	TTTGGGGATTTCATTGTCCACTGTTGGTCTCTTG CAGAGAC <u>G</u> CCCGTCCCATTCCGGAGCTCGATG TCGCGAGGCCGAGGGATTGGCCCTGGATGAT GAAGATGTGGAG
Oligonucleotide donor #2†	MCM2-R generation	TTTGGGGATTTCATTGTCCACTGTTGGTCTCTTG CAGAGACT <u>A</u> CCGTCCCATTCC <u>T</u> GAGCTCGATG TCT <u>A</u> CGAGGCCGAGGGATTGGCCCTGGATGAT GAAGATGTGGAG
Primer #1 (forward)	MCM2-2A and MCM2-R genotyping	ATCTAGAGGAAGCACTGGCCAC
Primer #2 (reverse)	MCM2-2A and MCM2-R genotyping	GAAGTTCTTGAAGCGGTGGTGG
Primer #3 (forward, for sequencing)	MCM2-2A and MCM2-R genotyping	CAGCAAGGACTTTGTAAGCCCG
Primer #4 (forward)	POLE4-KO genotyping	AAGGGGCCGAAATCGCG
Primer #5 (reverse)	POLE4-KO genotyping	TCCCCTTGCTTCAATGATGCC
Primer #6 (reverse, in deleted region)	POLE4-KO genotyping	GCAATCCTGTGTAGACGTGGAC

3  
4 \* 4 point mutations used to introduce Y81A and Y90A are underlined. Introducing the Y90A  
5 mutations disrupted the AccI restriction site, which was used as readout for genotyping.  
6 † 5 point mutations are underlined: 4 missense mutations to reverse A81 and A90 back to  
7 Y81 and Y90, 1 silent mutation to disrupt gRNA binding site.

## 1 Supplementary References

- 2 1 Flemr, M. & Buhler, M. Single-Step Generation of Conditional Knockout Mouse  
3 Embryonic Stem Cells. *Cell Rep* **12**, 709-716, doi:10.1016/j.celrep.2015.06.051  
4 (2015).
- 5 2 Cermak, T. *et al.* Efficient design and assembly of custom TALEN and other TAL  
6 effector-based constructs for DNA targeting. *Nucleic Acids Res* **39**, e82,  
7 doi:10.1093/nar/gkr218 (2011).
- 8 3 MacLean, B. *et al.* Skyline: an open source document editor for creating and  
9 analyzing targeted proteomics experiments. *Bioinformatics* **26**, 966-968,  
10 doi:10.1093/bioinformatics/btq054 (2010).
- 11 4 Petryk, N. *et al.* Genome-wide and sister chromatid-resolved profiling of protein  
12 occupancy in replicated chromatin with ChOR-seq and SCAR-seq. *Nat Protoc* **16**,  
13 4446-4493, doi:10.1038/s41596-021-00585-3 (2021).
- 14 5 Petryk, N. *et al.* MCM2 promotes symmetric inheritance of modified histones during  
15 DNA replication. *Science* **361**, 1389-1392, doi:10.1126/science.aau0294 (2018).
- 16 6 Lun, A. T. & Smyth, G. K. csaw: a Bioconductor package for differential binding  
17 analysis of ChIP-seq data using sliding windows. *Nucleic Acids Res* **44**, e45,  
18 doi:10.1093/nar/gkv1191 (2016).
- 19 7 Hiratani, I. *et al.* Global reorganization of replication domains during embryonic stem  
20 cell differentiation. *PLoS Biol* **6**, e245, doi:10.1371/journal.pbio.0060245 (2008).
- 21 8 Orlando, D. A. *et al.* Quantitative ChIP-Seq normalization reveals global modulation  
22 of the epigenome. *Cell Rep* **9**, 1163-1170, doi:10.1016/j.celrep.2014.10.018 (2014).
- 23 9 Zhang, Y. *et al.* Model-based analysis of ChIP-Seq (MACS). *Genome Biol* **9**, R137,  
24 doi:10.1186/gb-2008-9-9-r137 (2008).
- 25 10 Chen, K. *et al.* Broad H3K4me3 is associated with increased transcription elongation  
26 and enhancer activity at tumor-suppressor genes. *Nat Genet* **47**, 1149-1157,  
27 doi:10.1038/ng.3385 (2015).
- 28 11 Li, Q., Brown, J. B., Huang, H. & Bickel, P. J. Measuring reproducibility of high-  
29 throughput experiments. *The Annals of Applied Statistics* **5**, 1752-1779, 1728 (2011).
- 30 12 Blackledge, N. P. *et al.* PRC1 Catalytic Activity Is Central to Polycomb System  
31 Function. *Mol Cell* **77**, 857-874 e859, doi:10.1016/j.molcel.2019.12.001 (2020).
- 32 13 Healy, E. *et al.* PRC2.1 and PRC2.2 Synergize to Coordinate H3K27 Trimethylation.  
33 *Mol Cell* **76**, 437-452 e436, doi:10.1016/j.molcel.2019.08.012 (2019).
- 34 14 Turberfield, A. H. *et al.* KDM2 proteins constrain transcription from CpG island gene  
35 promoters independently of their histone demethylase activity. *Nucleic Acids Res* **47**,  
36 9005-9023, doi:10.1093/nar/gkz607 (2019).
- 37 15 Zhu, A., Ibrahim, J. G. & Love, M. I. Heavy-tailed prior distributions for sequence  
38 count data: removing the noise and preserving large differences. *Bioinformatics* **35**,  
39 2084-2092, doi:10.1093/bioinformatics/bty895 (2019).
- 40 16 Jin, Y. & Hammell, M. Analysis of RNA-Seq Data Using TETranscripts. *Methods Mol*  
41 *Biol* **1751**, 153-167, doi:10.1007/978-1-4939-7710-9\_11 (2018).
- 42 17 Jin, Y., Tam, O. H., Paniagua, E. & Hammell, M. TETranscripts: a package for  
43 including transposable elements in differential expression analysis of RNA-seq  
44 datasets. *Bioinformatics* **31**, 3593-3599, doi:10.1093/bioinformatics/btv422 (2015).
- 45 18 Yu, G., Wang, L. G., Han, Y. & He, Q. Y. clusterProfiler: an R package for  
46 comparing biological themes among gene clusters. *OMICS* **16**, 284-287,  
47 doi:10.1089/omi.2011.0118 (2012).

1 19 Subramanian, A. *et al.* Gene set enrichment analysis: a knowledge-based approach for  
2 interpreting genome-wide expression profiles. *Proc Natl Acad Sci U S A* **102**, 15545-  
3 15550, doi:10.1073/pnas.0506580102 (2005).

4 20 Deng, Q., Ramskold, D., Reinius, B. & Sandberg, R. Single-cell RNA-seq reveals  
5 dynamic, random monoallelic gene expression in mammalian cells. *Science* **343**, 193-  
6 196, doi:10.1126/science.1245316 (2014).

7 21 Eckersley-Maslin, M. A. *et al.* MERVL/Zscan4 Network Activation Results in  
8 Transient Genome-wide DNA Demethylation of mESCs. *Cell Rep* **17**, 179-192,  
9 doi:10.1016/j.celrep.2016.08.087 (2016).

10 22 Macfarlan, T. S. *et al.* Embryonic stem cell potency fluctuates with endogenous  
11 retrovirus activity. *Nature* **487**, 57-63, doi:10.1038/nature11244 (2012).

12 23 Hojfeldt, J. W. *et al.* Accurate H3K27 methylation can be established de novo by  
13 SUZ12-directed PRC2. *Nat Struct Mol Biol* **25**, 225-232, doi:10.1038/s41594-018-  
14 0036-6 (2018).

15 24 Wu, K. *et al.* SETDB1-Mediated Cell Fate Transition between 2C-Like and  
16 Pluripotent States. *Cell Rep* **30**, 25-36 e26, doi:10.1016/j.celrep.2019.12.010 (2020).

17 25 Bulut-Karslioglu, A. *et al.* Suv39h-dependent H3K9me3 marks intact  
18 retrotransposons and silences LINE elements in mouse embryonic stem cells. *Mol*  
19 *Cell* **55**, 277-290, doi:10.1016/j.molcel.2014.05.029 (2014).

20 26 Stuart, T. *et al.* Comprehensive Integration of Single-Cell Data. *Cell* **177**, 1888-1902  
21 e1821, doi:10.1016/j.cell.2019.05.031 (2019).

22 27 He, J. *et al.* Identifying transposable element expression dynamics and heterogeneity  
23 during development at the single-cell level with a processing pipeline scTE. *Nat*  
24 *Commun* **12**, 1456, doi:10.1038/s41467-021-21808-x (2021).

25 28 Bellelli, R. *et al.* Polepsilon Instability Drives Replication Stress, Abnormal  
26 Development, and Tumorigenesis. *Mol Cell* **70**, 707-721 e707,  
27 doi:10.1016/j.molcel.2018.04.008 (2018).

28